Binary blazed grating based on autostereoscopic display mechanism

Chien-Yue Chen,[1,*] Qing-Long Deng,[2] Donyau Chiang,[3] and Yao-Ru Chang[1]

[1]Graduate School of Optoelectronics, National Yunlin University of Science &Technology, 64002 Douliou Yunlin, Taiwan

[2]Institute of Photonic Systems, National Chiao Tung University, Tainan 71150, Taiwan

[3]Instrument Technology Research Center, Hsinchu 30076, Taiwan

*Corresponding author: chencyue@yuntech.edu.tw

Received 28 September 2011; revised 9 December 2011; accepted 9 December 2011;
posted 12 December 2011 (Doc. ID 155211); published 27 February 2012

The diffractive optical element blazed grating is proposed as the beam splitter for autostereoscopic displays in this study. With Lithographie Galvanoformung Abformung and inductively coupled plasma reactive-ion etching, a four-level blazed grating structure is produced. Moreover, highly translucent polydimethylsiloxane is transformed into symmetrical four-level blazed grating films. The experimental results show that the film can successfully transmit the left and the right images to the accurate positions, and the diffraction efficiency is 70.4% and the contrast ratio is above 80%, presenting the original stereoscopic image without it being affected by brightness and crosstalk. In the experiment of stereoscopic imaging, both the left and the right images could be clearly acquired, which proves the feasibility of blazed gratings as practical for the beam splitter of autostereoscopic displays.

OCIS codes: 050.1970, 120.2040, 230.1950.

1. Introduction

Both lenticular and parallax barriers are commonly utilized for spatial-multiplexed technology for stereo vision [1–3]. Generally speaking, the two technologies respectively utilized lenticular films and gratings on flat-panel displays for spectroscopic effects so that the left stereoscopic image is transmitted to the left eye and the right stereoscopic image is delivered to the right eye so that the viewers can view stereoscopic images without wearing three-dimensional (3D) glasses. It is therefore named autostereoscopic display technology [4], which not only changes the traditional way of viewing stereoscopic images but also provides a two-dimensional/3D switchable device for viewers to switch the mode. Nonetheless, with the accurate alignment of lenticular films, the roughness of the lens surface would result in dispersion or crosstalk [5]. On the other hand, the nontransparent area of grating spectroscopic films reduces four-fifths of the brightness of the entire panel [6], and the column arrangement is likely to appear moiré on the original LCD panel [7,8]. To overcome the above problems, Chen *et al.* proposed the concept of recycling and reusing the light, which enhances brightness of traditional stereoscopic technology with parallax barriers by 43% [6]. However, the entire brightness still could not reach the brightness standards for flat-panel displays [9]. Chen *et al.* further utilized the diffractive optical element, blazed grating, as the beam splitter for stereoscopic displays in 2010. With eight-level blazed gratings, which presented up to 82% diffraction efficiency and symmetrical arrangement, the problems in traditional binary gratings and lenticular films, such as insufficient brightness and dispersion, were replaced [10]. Su *et al.* successfully separated the left and the right images with holographic optical elements for spectroscopic gratings and proved the feasibility

1559-128X/12/070877-06$15.00/0

of diffraction spectroscopic technology in 2011. Nevertheless, the production of holographic films was rather complex, and the performance of the diffraction efficiency was merely 43% [11] so that it could not effectively improve the problem of insufficient brightness.

For this reason, aiming at the design of having blazed gratings on stereoscopic beam splitter, proposed in 2010, a symmetrical four-level blazed grating was produced. With the included angle of the symmetrical positive-one order diffraction to be the included angle for viewing the panel, the left and the right images were independently transmitted to both eyes in order to minimize the crosstalk [12]. In the experiment, Lithographie Galvanoformung Abformung (LIGA) [13] and inductively coupled plasma reactive-ion etching (ICP-RIE) [14] were utilized for etching on the four-level structure through two photomasks. Later on, the highly translucent material, polydimethylsiloxane (PDMS) (Sylgard 184, $n = 1.43$) [15–17], was selected for transforming into the mold. After the experiment, the symmetrical four-level blazed grating film was attached on the stereoscopic image so that the left and the right images were immediately transmitted to different positions, which were the distance for viewing stereoscopic images. Moreover, the maximum diffraction efficiency of the film being 70.4% and the contrast of crosstalk above 80.0% broke through the sufficient brightness of parallax barriers. Another benefit was that the size was less than the size of lenticular films. That makes it possible for implemented blazed grating to be used as the beam splitter for autostereoscopic display technology.

2. Experiments

A. Design of Blazed Grating

For separating the odd and the even pixels of the stereoscopic image, the pitch of the blazed grating should correspond to the subpixels of the panel and should be arranged with symmetrical pairs. In the experiment, a 2.2 in. thin-film transistor LCD (176 × 220 quarter video graphics array) with subpixel 66 μm was selected as the initial condition. The viewing distance of the stereoscopic image on the 2.2 in. panel was 120 cm, and the binocular distance was 6.54 cm. The included angle of the positive-one order diffraction was defined as the included angle for viewing so that the left and the right images could be separated. Furthermore, the design was based on monochromatic light ($\lambda = 532$ nm) in order to prove the feasibility of the experiment. With Eqs. (1) and (2), the diffraction angle and the pitch of the diffractive optical element (DOE) for positive-one order diffraction were calculated, as shown in Fig. 1:

$$\theta_m = \arctan[(a + b)/2D], \tag{1}$$

$$m\lambda = T \times n \times \sin\theta_m, \tag{2}$$

where a is the binocular distance, b the panel width, D the viewing distance, θ_m the diffraction angle at m level, T the pitch of blazed grating, n the refractive index of material of blazed grating, and λ the wavelength 532 nm.

B. Fabrication of Blazed Grating Film

With Eq. (2), the minimum pitch T of the blazed grating was obtained 8 μm. The minimum etching line width was 1.7 μm in this experiment. The blazed grating was produced with a four-level structure. According to [10], the maximum diffraction efficiency of four-level blazed gratings was around 79.0%. In regard to the experimental process, LIGA and ICP-RIE etching processes were utilized, and silicon wafer was the material substrate on which the symmetrical four-level blazed grating structure was etched. In this case, two photomasks were required for etching. In the process of ICP-RIE, the frequency

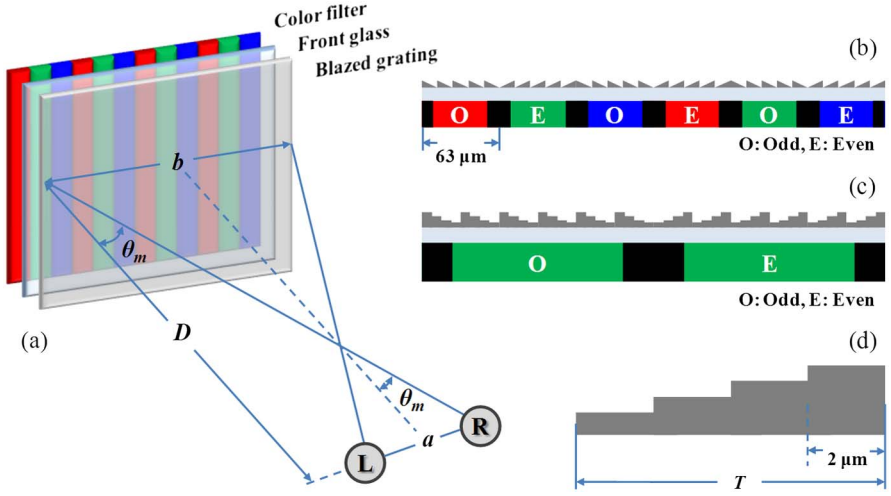

Fig. 1. (Color online) (a) Diffraction autostereoscopic display technology; (b) symmetrical pairs of the odd and the even pixels of the blazed grating; (c) symmetrical four-level blazed grating corresponding to the subpixel (532 nm); (d) structure of the single four-level blazed grating.

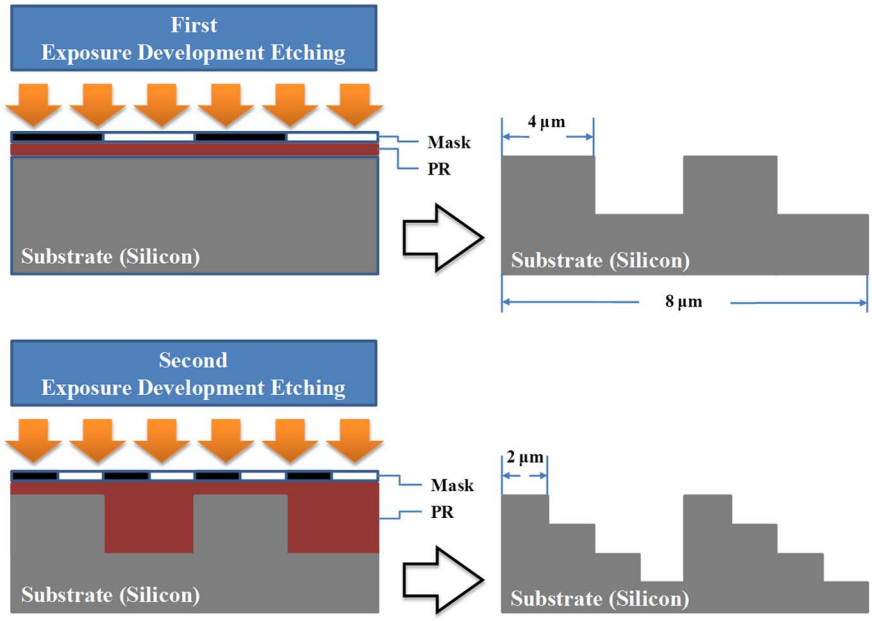

Fig. 2. (Color online) Two etching procedures. PR, photoresist.

for both the upper and the bottom electrode coils in the mechanism was 13.56 MHz radio frequency, and the chip cooling method with backside helium cooling was utilized. When fluoride ion plasma was acquired from ionizing SF_6, there was spontaneous adsorption between the fluoride ion plasma and the silicon substrate to generate a gaseous SiF_x compound. With vacuum gas to remove silicon substrate, as well as to protect the gaseous C_4F_8 from being ionized into CF_x, a protective film on CF_2 was generated [14]; the figure corresponding to the photomask was further etched with cycle reactions, as shown in Fig. 2.

Having successfully etched the four-level blazed grating (Fig. 3), an ionic sputter was utilized for coating a 300 Å thick nickel conducting layer on the structure; a high-intension and high-hardness Ni–Co alloy, about 200 μm thick, was electroformed for impact and abrasion resistance; and iron amino acid and cobalt sulfamate were utilized for lower internal stress [18]. After completing the electroforming, it was etched with KOH (30 wt. %) at 70 °C–80 °C for 4 h until the silicon substrate around the figure was completely etched for the complete mother mold. Table 1 shows the surface profile of the grating, which was measured with a 3D laser scanning microscope (VK-X200, KEYENCE Corp.). Finally, highly translucent PDMS was selected as the material for molding the symmetrical four-level blazed grating film.

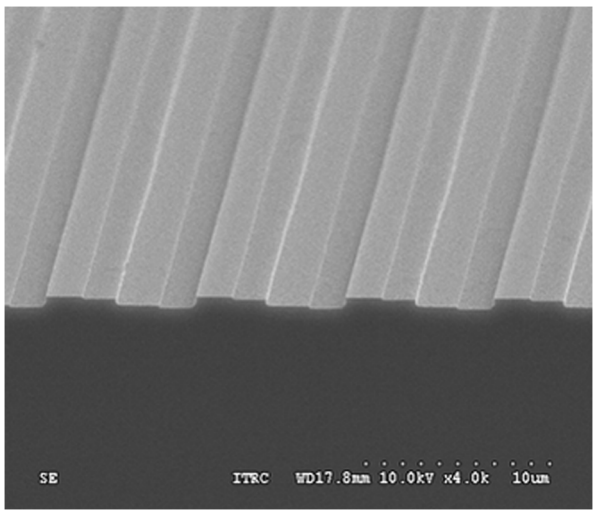

Fig. 3. Scanning electron microscope image of four-level blazed grating etching.

C. Results of Optical System

Figure 4 shows the optical measuring system for diffraction efficiency of blazed grating. A 532 nm green laser plane wave was applied as the backlight; a detector was placed at the position of the screen to measure the light of the left and the right positive-one order diffraction separated by the symmetrical four-level blazed grating film; and the diffraction efficiency was calculated with Eq. (3). The results showed that the efficiency of the right viewing angle of the positive-one order diffraction was 70.4%, while the efficiency of the left viewing angle of the positive-one order diffraction was 64.6%.

$$\eta = [I_{\text{out}}/(I_{\text{in}}/2)] \times 100\%. \quad (3)$$

Figure 5 displays the structure to prove the spectroscopic feasibility of images. First, aiming at the alignment for the placing of four-level blazed grating, the four corners of the blazed grating film were attached on the LCD, the aligned key accurately corresponded to the relative positions of the left and the right subpixels. The LCD presented the interlaced figure of the left and the right images, where the

Table 1. Surface Profile Data of the Grating

	Step 1	Step 2	Step 3	Step 4	Total	Design	Fabrication Error
Horizontal dist. (μm)	1.91	2.10	1.91	2.10	8.02	8.00	0.25%
High dist. (μm)	0.251	0.416	0.706	0.837	0.837	0.850	1.53%

odd subpixel was defined as the left image L and the even subpixel as the right image V. After the straight green light plane wave passed through the LCD and the blazed grating film, the left and the right spectroscopic images would be acquired on the screen, in which the left viewing angle appeared L and the right viewing angle showed V, and crosstalk did not appear on the two images. Moreover, when the image was changed to a stereoscopic image, the correct left and right images would be viewed from the viewing distance of 120 cm (Fig. 6). The image resolution is 176 × 220, and the contrast ratio is the same as Fig. 5.

3. Discussion

A. Fabrication Effect

The proposed symmetrical blazed grating film was produced with LIGA and ICP-RIE. Since both the minimum etching width of 1.7 μm and the structure depth of 850 nm were in the submicrometer range [19,20], a four-level structure was the limit etching close to the blazed grating. The highest diffraction efficiency, therefore, was 79.0% [10]. Moreover, the nonisotropic etching was protected from the cycle with SF_6 and C_4F_8 so that a vertical step structure was etched. Although the measured maximum diffraction efficiency was 70.4%, merely 8.6% different from the value in the theory, the factor might have resulted from the shrinkage and the residual stress of the material in the transforming process; however, it would not affect the left and the right spectroscopic effects.

B. Optical Effects

The measured left and right diffraction efficiency was 64.6% and 70.4%, respectively, as shown in Fig. 4. In regard to brightness, it was 22.4% higher than the brightness of traditional stereoscopic panels with parallax barriers and 43.0% higher than those with

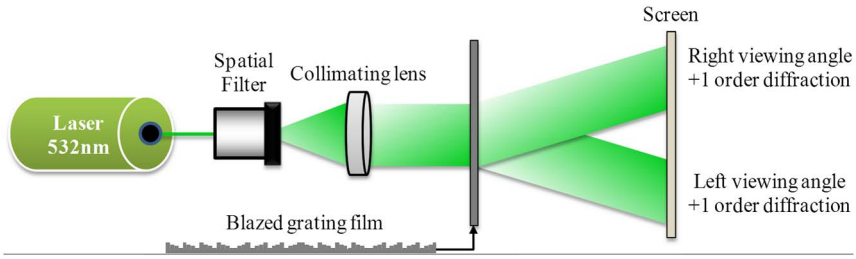

Fig. 4. (Color online) Optical measuring system.

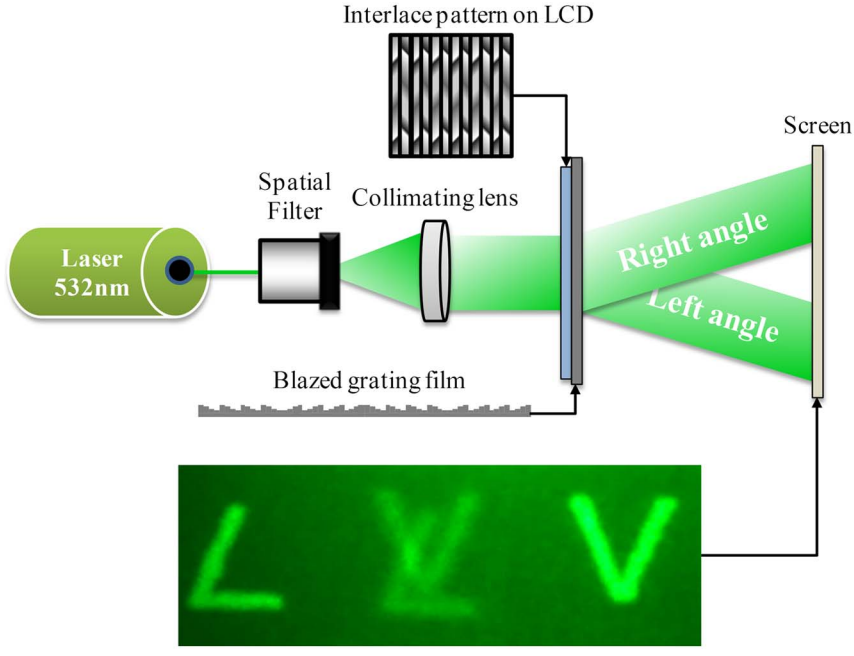

Fig. 5. (Color online) Left and the right spectroscopic images.

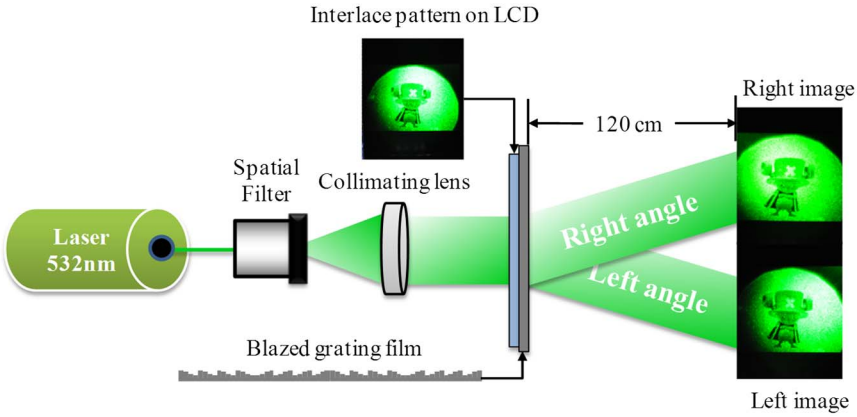

Fig. 6. (Color online) Spectroscopic outcome of stereoscopic images.

high brightness [6]. Even the holographic spectral component with holographic optical element (HOE) presented merely 43.0% diffraction efficiency [11]. In this case, 30% backlight was required for the original brightness. Although the 16-level and above approximate blazed grating structure or the original blazed grating could reach near 100% diffraction efficiency [21], the production cost and the difficulty would relatively increase.

Crosstalk in stereoscopic images depends on the contrast ratio (CR) of two images; that is, the image viewed by the left eye would not be affected by the one viewed by the right eye, and vice versa. The standard of CR is defined as 10% that crosstalk would seriously affect the stereoscopic image when the left and the right images interfere with each other, and the CR is lower than the standard [22], as shown in the following equation:

$$\mathrm{CR} = \frac{(L_{\max} - L_{\min})}{(L_{\max} + L_{\min})} \times 100\%. \tag{4}$$

The CR of crosstalk should be separately measured. In terms of the diffraction intension of the left viewing angle, a photomask was first covered the even pixels (right image) to measure the positive-one order diffraction intension ($L_{\max}$) of odd pixels. Then the odd pixels (left image) were covered to measure the diffraction intension ($L_{\min}$) interfered with by even pixels. Equation (4) could further calculate the CR of the left viewing angle. Contrarily, the CR of the right viewing angle was calculated with the positive-one order diffraction intension of even pixels and the diffraction intension interfered by odd pixels, as illustrated by Table 2. The CRs for the left and right viewing angles were 82.9% and 87.3%, respectively, which were larger than the defined standard and higher than the CR, 76.5%, of spectral components produced by the HOE [11], illustrating that the spectroscopic effects of diffraction optical elements were better than those of HOEs. Besides, L and V were separately transmitted to the left and the right eyes through the blazed grating, and no interference appeared in between them, as shown in Fig. 5.

Table 2. CR of the Left and the Right Viewing Angles

	$L_{\max}$	$L_{\min}$	CR
Left view	6.73 μW	0.63 μW	82.9%
Right view	8.53 μW	0.58 μW	87.3%

4. Conclusions

This study successfully applied the DOE, blazed grating, to the beam splitter in autostereoscopic displays and produced symmetrical four-level blazed grating film with LIGA and ICP-RIE. The experimental results showed that the left and the right stereoscopic images would be immediately separated to the corresponding left and right eyes through the blazed grating film on the screen with good brightness (the maximum diffraction efficiency 70.4%) and crosstalk (the CR larger than 80%). Compared with traditional parallax barriers and HOEs, the uniqueness of the DOEs is presented. Moreover, the thickness of the film is less than lenticular films so that the size of the stereoscopic displays would be largely reduced. With embossing or injection molding technologies, the demands would be largely increased.

This work is supported by National Science Council of Taiwan under contract NSC 98-2221-E-224-007-.

References

1. F. E. Ives, "Parallax stereogram and process of making same," U. S. patent 725,567 (1903).
2. H. Morishima, H. Nose, N. Taniguchi, K. Inoguchi, and S. Matsumura, "Rear cross lenticular 3-D display without eyeglasses," Proc. SPIE **3295**, 193–202 (1998).
3. C. Berkel, "Image preparation for 3D LCD," Proc. SPIE **3639**, 84–91 (1999).
4. H. M. Ozaktas and L. Onural, *Three-Dimensional Television* (Springer, 2008).
5. V. V. Saveljev, J. Y. Son, B. Javidi, S. K. Kim, and D. S. Kim, "Moiré minimization condition in three-dimensional image displays," J. Disp. Technol. **1**, 347–353 (2005).
6. C. Y. Chen, M. C. Chang, M. D. Ke, C. C. Lin, and Y. M. Chen, "A novel high brightness parallax barrier stereoscopy

technology using a reflective crown grating," Microw. Opt. Technol. Lett. **50**, 1610–1616 (2008).
7. M. Okui, M. Kobayashi, J. Arai, and F. Okano, "Moiré fringe reduction by optical filters in integral three-dimensional imaging on a color flat-panel display," Appl. Opt. **44**, 4475–4483 (2005).
8. M. Salmimaa and T. Järvenpää, "3-D crosstalk and luminance uniformity from angular luminance profiles of multiview autostereoscopic 3-D displays," J. Soc. Inf. Disp. **16**, 1033–1040 (2008).
9. P. Downen, "A closer look at flat-panel-display measurement standards and trends," Inf. Disp. **22**, 16–21 (2006).
10. C. Y. Chen, Q. L. Deng, and H. C. Wu, "A high-brightness diffractive stereoscopic display technology," Displays **31**, 169–174 (2010).
11. W. C. Su, C. Y. Chen, and Y. F. Wang, "Stereogram implemented with a holographic image splitter," Opt. Express **19**, 9942–9949 (2011).
12. C. Y. Chen, Q. L. Deng, and H. H. Lin, "Design of a symmetric blazed grating sheet embedded in autostereoscopic display," Opt. Lett. **36**, 3422–3424 (2011).
13. E. W. Becker, W. Ehrfeld, P. Hagmann, A. Maner, and D. Münchmeyer, "Fabrication of microstructures with high aspect ratios and great structural heights by synchrotron radiation lithography, galvanoforming, and plastic moulding (LIGA process)," Microelectron. Eng. **4**, 35–56 (1986).
14. S. C. Chen, Y. C. Lin, J. C. Wu, L. Horng, and C. H. Cheng, "Parameter optimization for an ICP deep silicon etching system," Microsys. Technol. **13**, 465–474 (2007).
15. S. M. Azmayesh-Fard, E. Flaim, and J. N. McMullin, "PDMS biochips with integrate waveguides," J. Micromech. Microeng. **20**, 087002 (2010).
16. R. Horváth, L. R Lindvold, and N. B Larsen, "Fabrication of all-polymer freestanding waveguides," J. Micromech. Microeng. **13**, 419–424 (2003).
17. L. M. Hopkins, J. T. Kelly, A. S. Wexler, and A. K. Prasad, "Particle image velocimetry measurements in complex geometries," Exp. Fluids **29**, 91–95 (2000).
18. M. C. Chou, H. Yang, and S. H. Yeh, "Microcomposite electroforming for LIGA technology," Microsys. Technol. **7**, 36–39 (2001).
19. Y. Q. Fu, A. Colli, A. Fasoli, J. K. Luo, A. J. Flewitt, A. C. Ferrari, and W. I. Milne, "Deep reactive ion etching as a tool for nanostructure fabrication," J. Vac. Sci. Technol. B **27**, 1520–1526 (2009).
20. M. Mizuhata, T. Miyake, Y. Nomoto, and S. Deki, "Deep reactive ion etching (deep-RIE) process for fabrication of ordered structural metal oxide thin films by the liquid phase infiltration method," Microelectron. Eng. **85**, 355–364 (2008).
21. G. Swanson and N. B. Veldkamp, "Diffractive optical elements for use in infrared systems," Opt. Eng. **28**, 605–608 (1989).
22. C. Y. Chen, T. Y. Hsieh, Q. L. Deng, W. C. Su, and Z. S. Cheng, "Design of a novel symmetric microprism array for dual-view display," Displays **31**, 99–103 (2010).